Calcium-Binding Mechanism of Human Nonerythroid α-Spectrin EF-Structures†

Susanne Lundberg,‡,§ Alexei V. Buevich,‖ Ingmar Sethson,‖ Ulf Edlund,‖ and Lars Backman*,‡

Departments of Biochemistry and Organic Chemistry, Umeå University, S-901 87 Umeå, Sweden

Received December 27, 1996; Revised Manuscript Received March 31, 1997⊗

ABSTRACT: We have used circular dichroism and ^{1}H- and ^{15}N-NMR spectroscopy to investigate calcium binding to the two EF-hands of human nonerythroid or αII-spectrin. Comparison of the ^{1}H-NMR spectra from the peptide containing both EF-hands to the peptides containing the single EF-I and EF-II structures showed that both the structural and calcium-binding properties are significantly different. Further studies of the 121 amino acid peptide containing both EF-hands using circular dichroism and NMR showed that the binding of calcium ions induces conformational changes. To investigate the calcium-binding mechanism, the chemical shifts changes were recorded using multidimensional NMR spectroscopy during calcium titration. A total of 25 titration curves were obtained, each corresponding to the chemical shift changes of individual amino acid residues. The shapes of these titration curves were either hyperbolic or sigmoidal. Using factor analysis, two functions were extracted, one hyperbolic and one sigmoidal, which accounted for nearly all information present in the titration curves. By fitting the two functions to binding curves based on different binding models, we found that the binding mechanism is best described as sequential. Since the sigmoidal type was more pronounced in the titration curves corresponding to residues from the first EF-hand, we suggest that calcium binding to the first EF-hand is described by the sigmoidal function, and that the hyperbolic function describes calcium binding to the second EF-hand. Therefore, is seems likely that the second EF-hand must contain bound calcium before the first EF-hand can bind.

Calcium ions are crucial for development and survival of all eukaryotic organisms. Its regulatory function as a secondary messenger has been implicated during the initial fertilization of the egg cell as well as during differentiation and proliferation; involving processes such as cell growth, cell motility, and muscle contraction (Berridge, 1993; Payne & Rudnick, 1989; Pietrobon *et al.*, 1990). In most cases, the calcium signal is not acting directly on the target process but rather transmitted within the cell by certain intracellular receptor or regulatory proteins, like calmodulin or troponin C. Binding of calcium ions to these regulatory proteins induces a change in conformation and a subsequent switch of the protein into an active form, able to mediate the calcium signal to the target process (Strynadka & James, 1991; McPahlen *et al.*, 1991).

In these calcium receptor proteins, the dominant calcium-binding motif is a helix−loop−helix motif or a so-called EF-hand. In the EF-hand, the calcium ion is bound to a loop of 12 amino acid residues, and the calcium ion is coordinated in a pentagonal bipyramidal arrangement that involves 6 of these residues (Strynadka & James, 1989). The coordinates are often referred to according to their locations in the coordination sphere and therefore correspond to the X, Y, Z, −Y, −X, and −Z coordinates, respectively. In the conserved EF-hand (Kretsinger *et al.*, 1991), the residues in the X and −Z positions are invariant aspartate and glutamate, respectively. The residues in the X, Y, Z, −X, and −Z positions ligate the calcium ion through their oxygen-bearing side chains, whereas in position −Y the carbonyl oxygen is coordinating the calcium ion.

Spectrin and the spectrin-based membrane skeleton are important targets for several calcium-activated proteins. It is known that influx of calcium into neurons leads to activation of the proteolytic enzyme calpain (calcium-activated neutral protease) followed by degradation of spectrin and other cytoskeletal proteins (Siman *et al.*, 1989; Di Stasi *et al.*, 1991; Saido *et al.*, 1994). This process seems to be under dual control, as the presence of calmodulin makes spectrin more susceptible to proteolysis by calpain (Seubert *et al.*, 1987; Harris *et al.*, 1989, 1990). There are additional sites for calmodulin on spectrin, as erythroid or αIβI-spectrin, which lacks the calpain cleavage site and still is able to bind calmodulin, though with much less affinity than the non-erythroid or αIIβII-spectrin (Berglund *et al.*, 1986; Harris *et al.*, 1988; Björk *et al.*, 1995). Adducin, which promotes the association between spectrin and actin, is another protein that, like calpain, seems to be regulated by calmodulin as well as protein kinases A and C (Mische *et al.*, 1987; Hughes & Bennett, 1995).

There are several reports showing that spectrin is capable of binding calcium ions directly and thus would be able to function as a calcium receptor [reviewed by Backman (1996)]. In most cases, the binding is of low affinity with dissociation constants in the range of ∼150−400 μM (Lundberg *et al.*, 1992; Travé *et al.*, 1995b). However, others (Wallis *et al.*, 1994) have found that the horse isoforms of spectrin have much higher affinity with dissociation constants in the nanomolar range. The reason for this discrepancy is not known.

† This work was supported by grants from the Swedish Natural Research Council.

* Correspondence should be addressed to this author at the Department of Biochemistry, Umeå University, S-901 87 Umeå, Sweden. Phone: (+46)-90-16 58 47. Fax: (+46)-90-13 63 10. E-mail: lars.backman@chem.umu.se.

‡ Department of Biochemistry.

§ Present address: National Defense Research Establishment, Department of NBC defence, S-901 82 Umeå, Sweden.

‖ Department of Organic Chemistry.

⊗ Abstract published in *Advance ACS Abstracts,* May 15, 1997.

S0006-2960(96)03153-4 CCC: $14.00

In previous studies using recombinant peptides, we have localized the main calcium-binding activity to one of the two EF-hands present in the C-terminal part of α-spectrins. Although these EF-hands are highly conserved (Kretsinger *et al.*, 1991), their calcium-binding properties are different. When the EF-hands are studied separately, only the second EF-hand appears to bind calcium in the presence of magnesium. Binding to the first EF-hand appears to be nonspecific as magnesium abolishes the binding of calcium (Lundberg *et al.*, 1995).

Recently, the solution structures of the calcium-bound and calcium-free forms of an 84 amino acid recombinant peptide comprising the 2 EF-hands in α-spectrin have been reported (Travé *et al.*, 1995a). The structures indicate that binding of calcium causes the helices flanking the calcium-binding loop regions to change into a more open conformation with concomitant exposure of hydrophobic residues. Similar changes have been reported for other calcium-binding proteins in the EF-hand family, *e.g.* calmodulin (Babu *et al.*, 1985; Zhang *et al.*, 1995) and troponin C (Gagné *et al.*, 1995). However, the changes in spectrin appear to be less pronounced. Based on the calcium-free and calcium-bound forms of the peptide, a model was suggested in which calcium binding initially induces a conformational change in the first EF-hand that is subsequently transferred to the second EF-hand through side-to-side interactions between the helices.

In this study, we have extended the characterization of the calcium-binding properties of the EF-hands in α-spectrins. Far- and near-UV circular dichroism (CD),[1] respectively, has been used to identify the secondary and tertiary structure changes upon calcium binding. In a detailed study of the calcium-binding mechanism, we have used multidimensional nuclear magnetic resonance (NMR) spectroscopy to follow structural changes upon addition of calcium. The obtained results indicate that although the first EF-hand is inactive when expressed alone, both EF-hands appear to bind calcium when expressed together as a pair. In addition, the titration curves appeared differently, ranging from sigmoidal to hyperbolic curves. Computer-assisted analysis of the titration curves revealed the presence of two differently shaped binding isotherms, corresponding to the binding of the first and the second calcium ion.

MATERIALS AND METHODS

Expression and Purification of Recombinant Peptides. The clones hfSp-EF-I, hfSp-EF-II, and hfSp-EF-I+II and their corresponding expression products EF-I, EF-II, and EF-I+II were obtained using the pGEX-2T fusion protein expression system (Pharmacia Biotech) as earlier described (Lundberg *et al.*, 1995). When preparing the ^{15}N-labeled peptides, the clones were grown and expressed in minimal media M9 (Mårtensson *et al.*, 1995) with $^{15}NH_4Cl$ as the nitrogen source. The recombinant proteins were purified by affinity chromatography on glutathione−Sepharose (Pharmacia Biotech). Thrombin was used to cleave the fusion protein while still attached to the affinity matrix. After cleavage, thrombin was removed by benzamidine−Sepharose or inactivated by the addition of PMSF. With time, the 15 kDa EF-I+II peptide was degraded into 12 and 14 kDa peptides. To minimize the extension of degradation, all experiments were done within 1 week of purification.

The peptide was occasionally contaminated with a small amount of calcium, probably due to the presence of endogenous calcium in the cell extract. Therefore, when the calcium-free form of the peptide was going to be studied, EDTA was included during the initial steps of the purification. However, EDTA was omitted when peptides were purified for the calcium titration experiments since the calcium chelator was interacting with the peptides in a way that made complete removal of the chelator impossible. The amount of endogenous calcium was estimated by comparing the NMR spectrum with the corresponding spectrum of the calcium-free but EDTA-containing peptide. Since the amount of endogenous calcium usually was very low (<10% of the peptide concentration), it was not accounted for in the calcium titration experiments.

Prior to the binding studies, all peptides were extensively dialyzed against 10 mM Tris-HCl, pH 7.3. Protein concentrations were determined from the absorbance at 280 nm using calculated molar absorptivities (Gill & von Hippel, 1989). The purity of expressed peptides was routinely checked under denaturing conditions using a Tricine-based buffer system designed for separation of low-molecular-mass proteins (Schägger & von Jagow, 1987).

Circular Dichroism and Calcium Titration. CD was used to examine the secondary structure changes upon calcium titration of the EF-II and EF-I+II peptides. Far-UV (200−250 nm) and near-UV (260−320 nm) measurements were collected using a Jasco 720 equipped with a 0.2 mm path length cuvette. Protein concentrations were ∼50 μM and ∼0.2 mM in the far- and near-UV measurements, respectively. All measurements were performed in 10 mM Tris-HCl, pH 7.3, and the dilution effect caused by adding small volumes of the calcium solution during the titrations was accounted for in the calculations. All spectra were adjusted at a specific wavelength representing a region where no changes occurred.

NMR Spectroscopy and Calcium Titration. The samples for the NMR experiments were concentrated to 0.3−1.5 mM using Pall Filtron or Amicon concentrators (1 kDa cutoff). All samples were prepared in aqueous solution (5% D_2O) with 10 mM Tris-HCl at pH 7.3. In order to reduce dilution of the protein samples during the calcium titration experiments, stock solutions of different concentrations (2.5−1000 mM) of $CaCl_2$ were used. The sample was not diluted more than 20%, and the changes in concentration during titration were accounted for in the calculations. Calcium titration measurements were done in the presence of 100 mM KCl with or without 50 mM $MgCl_2$. For all titration points, 1D ^{1}H-NMR and 2D (^{1}H,^{15}N)-HSQC spectra were recorded.

The NMR measurements were done at 30 °C on a AMX2-500 Bruker spectrometer operating at a proton frequency of 500.13 MHz. The ^{1}H-NMR spectra were acquired using the WATERGATE pulse sequence (Piotto *et al.*, 1992).

The two-dimensional (^{1}H,^{15}N)-HSQC experiments on the ^{15}N-labeled samples were performed in the sensitivity-enhanced gradient selection method (Kay *et al.*, 1992). A

[1] Abbreviations: NMR, nuclear magnetic resonance; CD, circular dichroism; PMSF, phenylmethanesulfonyl fluoride; EDTA, ethylenediaminetetraacetic acid; Tris, tris(hydroxymethyl)aminomethane; kDa, kilodalton(s); ppm, part per million; HSQC, heteronuclear singel-quantum correlation; NOESY, nuclear Overhauser effect spectroscopy; TOCSY, total correlation spectroscopy; K_I and K_{II}, macroscopic dissociation constants; K_c, disproportionation equilibrium constant.

total of 100 complex points in t_1 (^{15}N) and 1024 complex points in t_2 (^{1}H) were acquired. The t_1 dimension was linear predicted to have 200 complex points. A zero-filling to 512 (in t_1) and 2048 (in t_2) complex points was used. A Lorentzian−Gaussian window function in the t_2 dimension and a $\pi/2$-shifted squared sine window function in the t_1 dimension were used prior to Fourier transformation.

The two-dimensional NOESY (Jeener *et al.*, 1979) and TOCSY (Braunschweiler & Ernst, 1983) experiments were performed in the TPPI mode (Marion & Wütrich, 1983). The water suppression was achieved by implementation of the WATERGATE method (Piotto *et al.*, 1992); 200 ms mixing time and 70 ms spin lock time were used in the NOESY and the TOCSY experiment, respectively. A total of 256 complex points in the t_1 dimension and 1024 complex points in the t_2 dimension were acquired; 16 or 32 scans per each t_1 point with 1−2 s delay between scans were used. The spectral width was 8333.3 Hz in both dimensions. A Lorentzian−Gaussian window function in the t_2 dimension and a $\pi/2$-shifted squared sine function in the t_1 dimension were applied prior to Fourier transformation.

The three-dimensional (3D) NOESY-HSQC and TOCSY-HSQC experiments were performed in the States-TPPI mode for the NOESY and TOCSY parts and in the gradient-enhanced selection mode for the HSQC part; 100 ms mixing time and 60 ms spin lock time were used in the NOESY-HSQC and TOCSY-HSQC experiments, respectively. The number of acquired complex points was 1024*64*16 in the t_3 (^{1}H), t_2 (^{1}H), and t_1 (^{15}N) dimensions, respectively. A total of 16 scans per increment and 1 s delay between the scans were used. Linear prediction and zero-filling in the indirect dimensions finally gave the matrix of 1024 × 256 × 64 complex points. The processing of the 3D spectra was performed by using the CCNMR software (CCNMR written by C. Cieslar, at the Max-Planck Institut für Biochemie in Martinsried, Germany) with the same window functions which were used in the corresponding 2D experiments.

Factor Analysis. Factor analysis of the titration data consisted of principal component analysis (Malinovski, 1991) and curve resolution. Principal component analysis can be used to check the dimensionality of the data set, but its interpretation is difficult because it forces the obtained factors to be orthogonal. Especially the components beyond the first one are difficult to explain. If the assumption can be made that the concentrations and titration profiles are positive and added linearly, the techniques of curve resolution can be used (Lawton & Sylvestre, 1971). A very simple but powerful curve resolution technique is the alternating least-squares method that was invented by the psychologists Carrol and Chang (1970) and Sands and Young (1980), but later also applied to chemical problems (Knorr & Futrell, 1979). This technique uses iterating least squares, in a way that each iteration step is followed by a removal of negative values (Karjalainen, 1989; Karjalainen & Karjalainen, 1996). With the knowledge previously obtained by principal component analysis, it is possible to get convergence into a solution:

$$D = p_1 f_1 + p_2 f_2 + ... + E$$

where D is the matrix of the titration curves; p_1, p_2, etc. are concentration profiles (only positive values allowed); f_1, f_2, etc. are the standardized elementary titration curves; and E is the residual, assumed to be random, noise. The expression above can also be written in a matrix notation as

$$D = PF'$$

From this equation, the least-squares solutions for P and F are

$$P = DF(F'F)^{-1}$$

$$F' = (P'P)^{-1}P'D$$

The algorithm starts by filling the matrix F with random values (or principal components of D). If convergence is reached and the residual is small and without obvious structure, the decomposition has succeeded.

The experimental data were separated into two groups. The first was represented by the curves which fulfilled the requirements of the algorithm, that is, the titration curves which were the sum of only positively defined functions and thus were constantly growing. The second group included curves represented by a sum of negatively and positively defined functions which consequently appeared to be not constantly growing. The curves containing missing data points were also included in the second group.

The factor analysis was done using the curves from the first group, and the functions extracted from this analysis were used to analyze the curves belonging to the second group. This was achieved by solving a system of linear equations which can be presented in a matrix notation:

$$P = DF'(FF')^{-1}$$

where D corresponds to the matrix of experimental titration data of the second group, F to the matrix of the two factors identified in the factor analysis, and P to the matrix of coefficients to be determined. All calculations were done by using MATLAB software (copyrighted by The MathWorks., Inc., Cochitaute Place, 24 Prime Park Way, Natick, MA 01760).

RESULTS

Expression and Purification. The localization of the recombinant peptides to the α-spectrin monomer as well as the amino acid sequence of the EF-I, EF-II, and EF-I + II peptides is outlined in Figure 1. Due to the nature of the expression system, the peptides contained three to six additional amino acid residues in the N- and C-termini, derived from the plasmid. These additional residues were not included in the numbering of the recombinant peptide. Therefore, amino acid residue number 1 refers to the first residue in the sequence originating from spectrin. The additional residues in the N- and C-termini were included when calculating the molecular weights and molar absorptivities of the recombinant products.

Neither of the EF-I, EF-II, or EF-I + II peptides were completely stable, as degradation products could be observed in minor amounts immediately after purification and more extensively with time. In the case of EF-I + II, two degradation products (12 and 14 kDa) appeared in significant amounts after several weeks of storage. Independently of the degradation level, the N-terminal part of the peptide (amino acid residues 8−81), including the two EF-structures, was easily identified in the NMR structural analysis, and appeared identical.

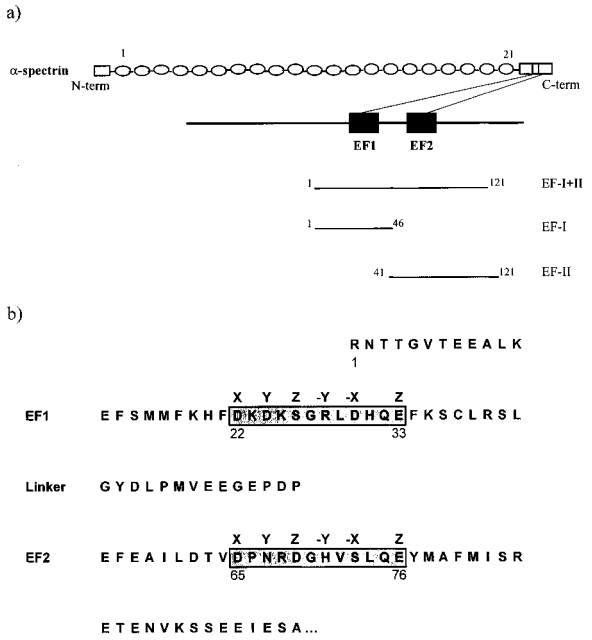

FIGURE 1: (a) Schematic structure of α-spectrin depicting the nonhomologous N- and C-termini and the 21 ∼106 amino acid residue repeats as well as the localization of peptides used in this study. Note that the amino acids in the EF-I and EF-II peptides are numbered according to how they are positioned in the EF-I + II peptide. (b) Amino acid sequences of the first 98 residue of the EF-I + II peptide. Both EF-hand sequences are in accordance with the established canonical EF-hand sequence (Kretsinger *et al.*, 1991). Also shown are the residues that correspond to the X, Y, Z, −Y, −X, and −Z ligands that make up the calcium coordination sphere. These residues, except for residue −Y, which ligates calcium through its backbone carbonyl oxygen, bind the calcium ion through their oxygen-bearing side chains. The residues comprising the calcium-binding loops are shaded, and the numbering is shown under the sequence.

It was observed that a small amount (<10%) of the EF-I + II peptide was already in the calcium-bound form immediately after purification. To achieve all expression products in the calcium-free form, EDTA was included during the initial stages of purification. However, it was found that it was not possible to remove all EDTA from the peptide despite extensive dialysis or gel filtration. We concluded that EDTA somehow interacts with the peptide, and therefore omitted the chelator when preparing samples for calcium titration.

CD and ^{1}H-NMR Spectroscopy of EF-I, EF-II, and EF-I + II. We have previously shown that the addition of calcium to the peptides containing either the first or both EF-structures does not have any effect on the far-UV CD, in contrast to the EF-II peptide that showed a significant increase in molar ellipticity at 220 nm, indicative of an increased α-helical content (Lundberg *et al.*, 1995). This was consistent with the finding that the EF-II peptide, but not the EF-I peptide, EF-structure was active in a calcium-binding assay. It is known that changes in the far-UV region primarily reflect changes in the secondary structures, whereas changes in the near-UV region are more dependent on the tertiary structure (Woody, 1995). Therefore, we extended the CD measurements to include the near-UV region. It was found that the spectrum was clearly dependent on the addition of calcium (Figure 2). This confirmed previous structural studies; upon calcium binding to EF-I + II, the secondary structure content is not changed, but instead the secondary structure elements are moved relative to each other (Travé *et al.*, 1995a).

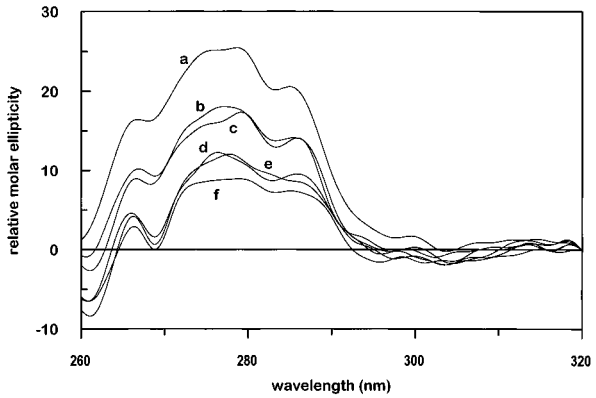

FIGURE 2: Near-UV CD spectra of EF-I + II at calcium:peptide ratios of 0:1 (a), 0.5:1 (b), 1:1 (c), 2:1 (d), 5:1 (e), and 10:1 (f). The concentration of EF-I + II was 183 μM in 10 mM Tris-HCl, pH 7.3.

That the structural changes upon calcium addition were significantly different depending on whether a single EF-hand or a pair were studied was confirmed by comparing the ^{1}H-NMR spectra of EF-I + II and EF-II (Figure 3). Independent of whether calcium was present or not, the amide proton chemical shift range of EF-II was significantly more narrow than that of EF-I + II, indicating that EF-II did not form the typical helix−loop−helix structure representative of an EF-hand. For instance, the conserved glycine located in the middle of the loop (Gly-27 and Gly-70 in EF-I and EF-II, respectively; see Figure 1) has a characteristic downfield chemical shift, which has been suggested to be due to strong hydrogen bonding through its amide proton to the calcium-ligating aspartate residue in the first position of the calcium-binding loop (Starovasnik *et al.*, 1993). The spectrum of EF-I + II contained the expected proton chemical shifts downfield of 10.0 ppm, whereas in the spectrum of EF-II no signals were observable downfield of 9.0 ppm (lower spectra in Figure 3). When calcium was added to the EF-I + II peptide, several signals corresponding to residues from both EF-hands changed their chemical shifts (Figure 3a). In particular, the characteristic chemical shifts of the glycines were both changed upon addition of calcium. In contrast, calcium had a significant different effect on the ^{1}H-NMR spectrum of the EF-II peptide. In this case, a few additional peaks in the amide region, as well as a redistribution of the resonances, were seen (Figure 3b). The low concentration and stability of the EF-I peptide complicated the NMR measurements of that peptide; however, we have not observed any changes in the proton spectra of EF-I upon calcium addition (data not shown). It is therefore apparent that the second, but not the first, EF-hand binds calcium when expressed alone.

Calcium Titration of EF-I + II. The detailed calcium-binding behavior of the EF-I + II peptide was studied by the effects of sequential calcium additions on the (^{1}H,^{15}N)-HSQC spectra of EF-I + II. Including magnesium chloride up to 50 mM did not affect the calcium titration; neither did magnesium titration have any significant effects on the chemical shift patterns (data not shown). The conformational changes observed when adding calcium were therefore likely to be a consequence of specific interactions between the EF-hands and calcium and not by other unspecific electrostatic interactions.

The sequential assignment of amino acids 5−85 was done using 3D NOESY-HSQC and 3D TOCSY-HSQC experi-

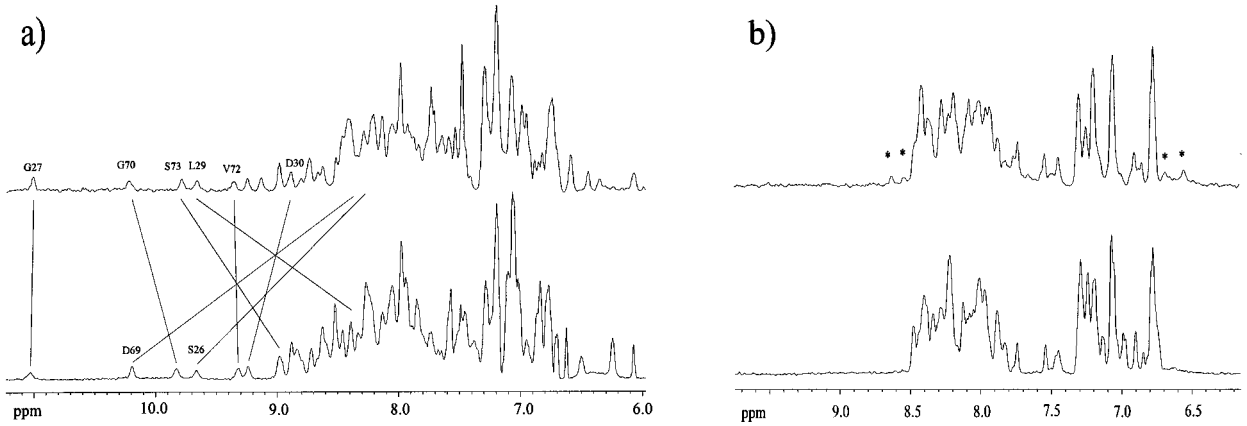

FIGURE 3: Amide region of ^{1}H-NMR spectra of EF-I + II (a) and EF-II (b). Bottom panels show the spectra obtained in the absence of calcium whereas the spectra in the top panels were obtained in the presence of 5 mM $CaCl_2$. In the spectra of EF-I + II, drawn lines indicate changes in the chemical shifts of assigned amino acid residues caused by calcium binding, and in the spectra of EF-II, asterisks indicate new signals appearing in the calcium-bound form of the peptide.

ments on ^{15}N labeled EF-I + II. The chemical shifts of the amide resonances and α-protons were identical to the corresponding resonances of chicken α-spectrin (Gilles Travé, personal communication), except for the 59th residue, which differs in the two isoforms (alanine in human αII-spectrin and serine in chicken α-spectrin).

We were able to follow the chemical shift changes of 25 residues. The signals of the remaining residues either were not fully resolved, did not change during titration or were significantly broadened due to an intermediate exchange rate. For 21 individual amino acids, the chemical shift changes of the amide protons were recorded, and for the remaining 4 residues, the chemical shift changes of the amide nitrogens were followed. The HSQC spectra of EF-I + II in the apo and calcium-bound forms are shown in Figure 4.

The shapes of the obtained titration curves are important when determining the binding mechanism. For instance, if both sites bind calcium independently, and with comparable binding strengths, all titration curves should be hyperbolic. As shown in Figure 5, the titration curves of the residues in the first EF-hand loop displayed both sigmoidal and hyperbolic titration curves, whereas those in the second EF-hand loop only showed the hyperbolic type. The presence of only hyperbolic chemical shift curves indicated that the binding of calcium to the second EF-hand is not dependent on any other sites. In contrast, due to the sigmoidal behavior of several residues of the first EF-hand, it seems apparent that the binding to the first site is dependent on the presence of calcium in the second EF-hand. Thus, it follows that the calcium binding appears to follow a sequential binding mechanism.

Computer-Assisted Analysis of the Titration Curves. In general, the binding of two ligands to a substrate can be described as

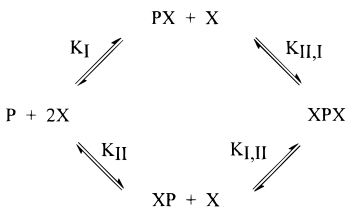

The different models of binding that can occur, together with a definition of the parameters used, are presented in the appendix. In order to determine the binding constants, the fractional saturation of the two sites has to be known.

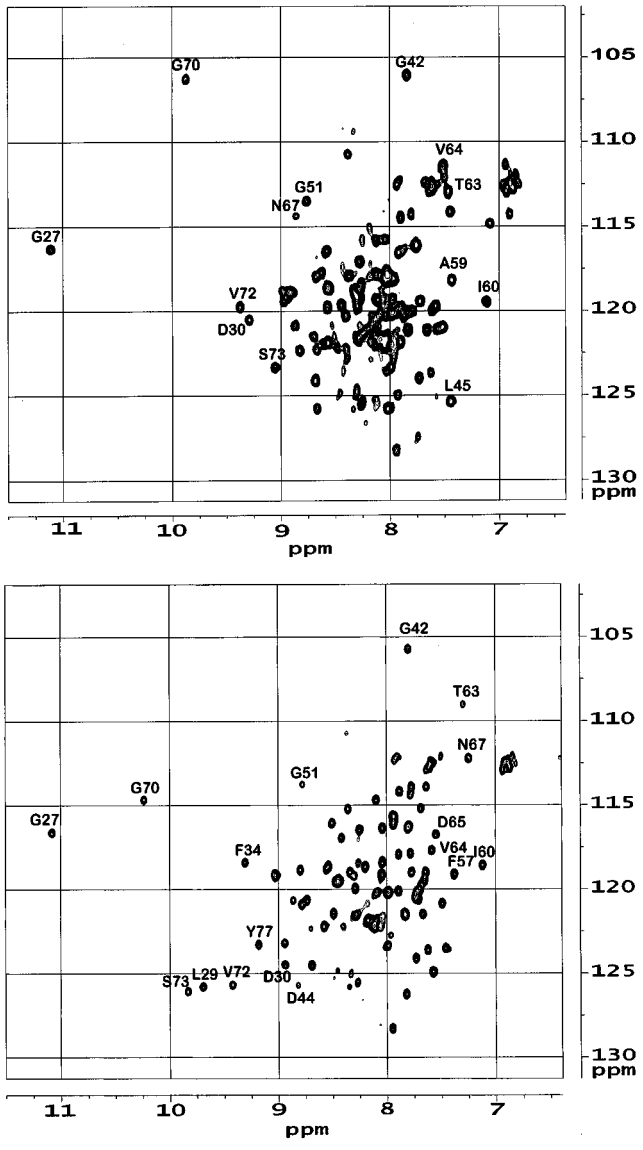

FIGURE 4: (^{1}H,^{15}N)-HSQC spectra of EF-I + II (0.5 mM in Tris-HCl, pH 7.3) in the absence (top) and presence (bottom) of 7.5 mM $CaCl_2$. By using 3D NOESY-HSQC and 3D TOCSY-HSQC, residues 5−85 were assigned. However, for clarity only a few of the assignments are shown.

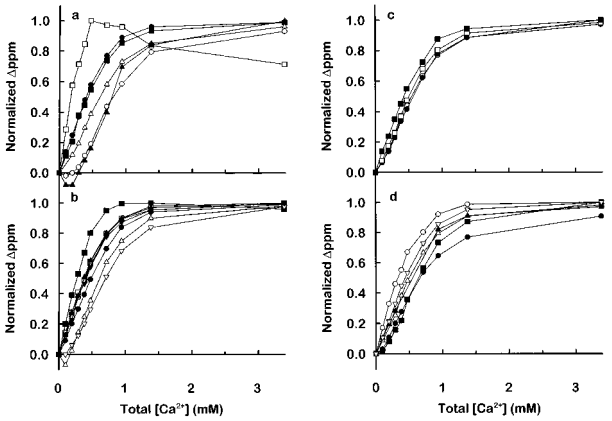

FIGURE 5: Calcium titration curves of the 25 amino acid residues that were possible to follow during titration. To facilitate comparison of the curve shapes, the normalized changes in chemical shifts are shown. (a) Residues found in the loop of the first EF-hand: (○) Asp-22, (●) Lys-23, (□) Gly-27, (■); Asn-30, (△) Gln-32, (▲) Glu-33. (b) Residues from the first EF-hand helices: (○) Phe-14, (●) Ser-15, (□) Met-17, (■) Phe-21, (△) Phe-34, (▲) Lys-35, (▽) Ser-36, (▼) Cys-37. (c) Residues from the loop of the second EF-hand: (○) Arg-68, (●) Gly-70, (□) Val-72, (■) Gln-75. (d) Residues found in the helices of the second EF-hand and the linker region: (○) Asp-44, (●) Leu-45, (□) Phe-57, (■) Ala-59, (△)Val-64, (▲) Ala-79, (▽) Glu-85.

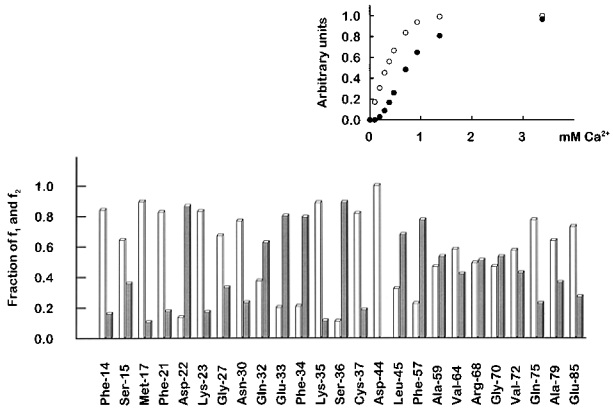

FIGURE 6: Bar representation of the relative proportions of f_1 (shaded) and f_2 (white) in each of the 25 titration curves. The shapes of f_1 (●) and f_2 (○) are inserted.

From the titration data for the EF-I + II peptide, it was apparent that even though a few titration curves appeared as either hyperbolic or sigmoidal, most curves appeared as intermediates, that is, a mixture of the two extreme cases. We assumed that the reason for that was that nearly all amino acids within the EF-I + II peptide were affected by calcium binding to both EF-hands. In order to extract the fractional saturations from the complicated set of titration curves, we used a factor analysis approach, which has earlier been shown to be successful in separating the pure effects from a complex set of data (Malinovski, 1991).

By definition of the curve resolution technique, the titration curves needed to be the sum of only positively defined functions. In order to fulfill the requirements of the algorithm, six titration curves were excluded in the first analysis. It was found that 97.7% of the information from the 16 remaining titration curves could be described by only 2 factors (f_1 and f_2). These factors displayed sigmoidal and hyperbolic shapes, respectively (Figure 6, insert). The second group of curves was analyzed using f_1 and f_2 factors, and it was found that the extracted functions were sufficient

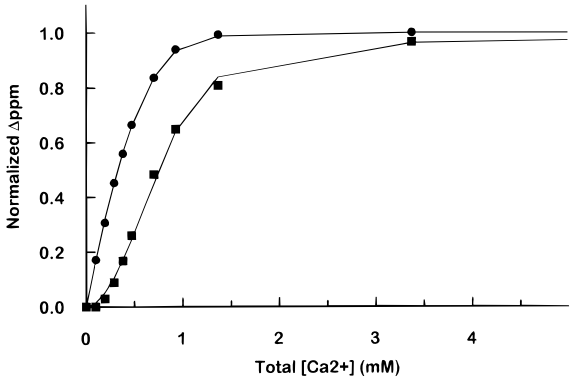

FIGURE 7: Two factors extracted from the factor analysis: (■) f_1 (sigmoidal); and (●) f_2 (hyperbolic). The solid lines represent the best fit obtained when fitting the two functions to a sequential binding model (K_I = 47.8 μM and K_{II} = 96.1 μM). An equally good fit was obtained when fitting the data to a cooperative binding model; in this case, K_I = 47.8 μM, K_{II} = 631.6 M, and K_C = 6.5 × 10^6.

to describe the shapes of these curves. A bar representation of the relative amounts of the 2 factors for the 25 titration curves is presented in Figure 6. f_1, the sigmoidal factor, contributed a larger amount to the titration curves of the residues located in the first EF-hand; the titration curves of Asp-22, Glu-33, and Phe-34 were all described to about 80% by the sigmoidal function. The titration curves of the residues within the second EF-hand could mostly be described by equal amounts of f_1 and f_2, indicating that this part of the structure was sensitive to interactions of both EF-hands with calcium. However, since the contribution of f_1 to the titration curves of the first EF-hand was significantly larger than to the titration curves of the second EF-hand, we believe that the sigmoidal function is representative of binding to the first EF-hand and the hyperbolic function describes calcium binding to the second EF-hand.

The two functions that could be extracted from the titration curves in the factor analysis were analyzed by fitting binding curves based on different models: sequential binding, cooperative binding, or two independent binding sites models as defined in the appendix. From the analysis, it was obvious that only a sequential or cooperative binding behavior gave rise to the observed curve shapes (Figure 7, solid line). The minimum error of sum of squares obtained for the sequential model was identical to that of the cooperative model but significantly less than for the two independent sites model. However, for the cooperative model, the K_{II} and K_c values indicated that the binding was approaching the sequential type. Therefore, it seems that the binding mechanism is best described by a sequential model.

Thus, we believe that the first EF-structure is incapable of binding calcium unless the second EF-hand is in a calcium-bound form. The dissociation constants for the two sites giving the best fit (the sequential binding model) were in the same range; ~96 μM and ~48 μM for the first and second EF-hand, respectively. These values are in reasonable agreement with previous measurements (Lundberg *et al.*, 1992; Travé *et al.*, 1995b).

DISCUSSION

Properties of the EF-Hand Pair Compared to the Single EF-I and EF-II Peptides. When comparing the EF-I and EF-II peptides to the complete EF-hand pair, it was found,

independently of the method used, that their stability, structural properties, and calcium-binding properties were different. The single EF-I and EF-II peptides, and in particular EF-I, showed a higher degree of degradation which occurred after only a few days of storage. In the case of the EF-I + II peptide, the NMR analysis showed that degradation occurred in the C-terminal region, keeping the EF-structures intact. The presence of a secondary thrombin cleavage site within the 40 amino acid C-terminal tail indicates that the degradation is a side-effect of the purification method used.

The structural properties were studied using ^{1}H-NMR. The peptide containing both EF-hands displayed the previously described chemical shift pattern of EF-hands, whereas the single EF-hands showed a more narrow chemical shift distribution. Previously, we have shown that the far-UV CD of EF-II , but not that of EF-I + II, is affected by calcium, indicating an increased α-helical content in EF-II upon calcium binding (Lundberg *et al.*, 1995). Additional CD measurements showed that calcium altered the near-UV region of EF-I + II, indicating that binding of calcium primarly caused tertiary structure changes in this peptide. Consistently, upon calcium addition, most of the proton chemical shifts from EF-I + II were altered. Adding calcium to EF-II resulted in less pronounced changes, whereas we have not detected any effect of calcium on either the CD or the ^{1}H-NMR spectra of EF-I. The results indicate that both EF-hands bind calcium in the EF-hand pair, whereas when expressed separately only the second EF-structure appears to be active. However, it should be noted that the low stability and low concentration attainable of EF-I made interpretation difficult. Therefore, the lack of binding to EF-I may be due to improper folding.

The importance of interplay between the two EF-hands within a pair has been shown for EF-structure-containing proteins such as calbindin, calmodulin, and troponin C. The presence of positive cooperativity has been reported for calbindin (Linse *et al.*, 1991) and calmodulin (Pedigo & Shea, 1995) and a stepwise binding behavior for the regulatory domain of troponin C (Li *et al.*, 1995). In this study, we have again revealed the importance of cross-talk between two EF-hands to obtain the calcium-binding properties of an EF-hand pair.

Calcium Binding to the EF-I + II Peptide. (A) Calcium Titration of EF-I + II in the Absence and Presence of $MgCl_2$. We have used 2D (^{1}H,^{15}N)-HSQC spectra to investigate the binding of calcium ions to the two EF-hands in human αII-spectrin. From the calcium titration experiments, we were able to extract 25 different titration curves corresponding to different amino acids from both EF-structures as well as the linker region. Magnesium titration of EF-I + II did not result in any similar chemical shift changes. Even though minor changes in the spectra were observed, they were small compared to the changes observed during calcium titration, and no saturation point could be reached despite adding magnesium chloride up to 50 mM. Furthermore, the presence of 50 mM $MgCl_2$ did not affect the calcium titration curves. The results show that although magnesium ions are interacting with the EF-I + II peptide, the binding is clearly different from that of calcium ions and probably more unspecific. We have previously shown (Lundberg *et al.*, 1992) that the presence of magnesium reduces the affinity of spectrin for calcium about 3-fold. While not competing directly with the calcium ions, the unspecific binding of magnesium is likely to reduce the negative charge of the surface, therefore also reducing the calcium affinity.

(B) Analysis of the Titration Curves. At least two effects should contribute to the titration curves, that is, the specific association of calcium with the two EF-hands. The observed diversity in the shapes of the titration curves indicated that different parts of the EF-hands responded differently to the presence of calcium ions, and that most residues sensed the calcium binding to both EF-hands. Before it was possible to distinguish between plausible binding models, it was therefore necessary to clarify the data in order to extract the functions giving rise to the observed shapes. In this type of analysis, it was also possible to reveal both the presence and the amount of additional effects as, for instance, structural changes due to unspecific electrostatic interactions.

To define which type of curve shapes contributed to the observed data, factor analysis was used. By this analysis, it was possible to define the minimal number of factors (isotherms). It was found that all curves could be described by two factors which had either a sigmoidal or a hyperbolic shape. Using the extracted binding isotherms, we analyzed the data further by fitting binding curves based on different binding models. With a two-site independent model, it was not possible to obtain the observed curve shapes, whereas the sequential binding model and the extreme case of the positive cooperative binding model ($K_I = \sim 48\ \mu$M, $K_{II} = \sim 631$ M, $K_C = \sim 6.5 \times 10^6$) fitted equally well to the binding data. Therefore, it was not possible to distinguish between these two binding models. However, due to the large disproportionation equilibrium constant (K_c), the sequential and cooperative models do in fact describe the same type of binding.

The best fit of the sequential binding model to our binding data occurred at dissociation constants of ∼96 μM and ∼48 μM for the first and second EF-hands, respectively. These values are in reasonable agreement with binding data obtained for the chicken and calf brain nonerythroid α-spectrin isoforms (Lundberg *et al.*, 1992; Travé *et al.*, 1995b), which is expected since the EF-hands in these two isoforms have identical or nearly identical amino acid sequences.

(C) Calcium-Binding Mechanism of EF-I + II. The relative proportions of the two extracted factors (hyperbolic and sigmoidal) for all titration curves are shown in Figure 7. A comparison of the titration data for the two binding loops shows that only residues from the first EF-hand gave rise to sigmoidal titration curves (residues 22, 33, 34, and 36) whereas all residues in the second EF-hand that we were able to identify displayed a mixture of two effects. Because of that, we found it reasonable to assume that the sigmoidal curve showed the behavior of the first EF-hand (EF1), and, consequently, the hyperbolic titration curves displayed the calcium-binding behavior of the second EF-hand (EF2). By correlating the shape of titration curve to the interactions made by the particular amino acids, we found that most residues from EF1 that exhibit the hyperbolic type of titration curve are interacting with either the loop region or the helices of EF2. The consequence might be that those residues respond to structural changes caused by calcium binding to EF2. For instance, the titration curve of Ser-36 was of the sigmoidal type, whereas those of Lys-35 and Cys-37 were hyperbolic (Figure 5). These residues are located in the second helix of EF1, in which Lys-35 and Cys-37 are

interacting with the EF2 residues Phe-57 and Tyr-77, respectively. In contrast, the Ser-36 residue is not interacting with any residue from the second EF-structure. Therefore it seems likely that the second EF-hand binds calcium first, inducing conformational changes that render the first EF-hand capable of binding calcium. However, since all residues (with the exception of the linker residue Asp-44) display titration curves containing contributions from both factors, we cannot at present exclude the possibility that EF1 binds first, as the structural study of Travé *et al.* (1995a) indicates. It may even be possible that both sites bind calcium simultaneously and that the binding induces a immediate conformational change of EF2 whereas the changes in EF1 somehow are delayed. From the amino acid sequence of the two EF-hands, it is not possible to explain why the first EF-structure is more restricted in its calcium-binding activity since both are highly conserved (Kretsinger *et al*., 1991). However, the solution structures of unbound and calcium-bound EF-I + II reveal several noticeable features of the two EF-hands. In the apo form, the binding loop of EF2 appears to contain no internal interactions. In contrast, in the calcium-bound form of EF2, the loop has closed, and especially the edges of the loop are closer together (the distance between the side chain oxygens of Asp-65 and Glu-76 is 10.8 Å in the apoform, whereas in the calcium-bound form it is 4.0 Å). The loop of the first EF-hand is more closed in the apo form. Specifically, two interactions, the salt bridge between Lys-23 and Glu-33 and the hydrophobic interaction between Met-17 and Leu-41, are disrupted upon calcium binding and thus might be crucial for the closed-to-open transition. The consequence of the Lys-23/Glu-33 salt bridge is that the calcium-ligating aspartate in the first position of the loop is pointing outward from the loop, and should therefore be less accessible for ligating calcium. Our data show that the titration curves corresponding to Lys-23 and Met-17 are both hyperbolic, indicating that these residues respond mainly to calcium binding to the second EF-structure.

We therefore suggest that calcium binding to EF2 closes the loop and thus reorients the EF2 helices from the almost parallel orientation observed in the apo form to the perpendicular state seen in the calcium-bound form. The conformational changes in EF2 are then mediated to the helices belonging to EF1, and as a consequence, interactions within EF1 are broken. The loop of the first EF-hand is now allowed to reorient in order to obtain a more favorable calcium-binding form.

It is obvious that our results do not support all features of the "motor-transistor" model of Travé *et al.* (1995a). Based on structural analysis of the calcium-free and calcium-bound forms, they proposed that the binding of calcium to EF1 induces conformational changes in this binding loop that are propagated to EF2. In their model, EF1 functions as the motor, generating the movement, whereas EF2 acts as a transistor, unable to generate movement but able to modulate the calcium affinity of both EF1 and EF2 through cooperative effects.

The β-sheet formed by a few residues located in the middle of each loop of the two EF-hands has previously been suggested to be important for the cross-talk between EF-hands (Zhang *et al*., 1995). The residue−residue distance plots of the calcium-free and calcium-bound forms of EF-I + II (Travé *et al.*, 1995a) show that there are more contacts forming the β-sheet of the EF-hands in the calcium-free form than in the calcium-bound form. These interactions might provide another explanation for the suppressive effect the calcium-free form of the second EF-hand appears to have on the first EF-hand. As EF2 binds calcium, the subsequent closing of the loop might result in a reduction in β-sheet contacts and thus a conformational change in the loop of EF1. At this stage, it is not possible to determine whether the β-sheet contacts or the contacts between the helices are most important. It is likely, however, that both types of interactions are of importance, since as shown in Figure 7 both EF1 residues in the β-sheet (Asn-30) and α-helical residues (Lys-35, Cys-37) that interact with helices from EF2 display titration curves in which the main contributions come from effects caused by the second EF-structure.

(D) Physiological Significance of Calcium Binding to Spectrin. The calcium binding to spectrin is unusually low for EF-hand proteins, and it has been questioned if the binding is occurring *in vivo* (Linse & Forsén, 1995; Chazin, 1995). In excitable cells, the calcium concentration has been suggested to be much higher than was previously believed (Clapham, 1995). Also, the calcium ions are not evenly distributed in the cell upon influx; instead, calcium sparks and waves are observed. It is therefore possible that, close to the plasma membrane of nerve cells, where spectrin is concentrated, the calcium concentration may reach such levels that a substantial fraction of the calcium-binding sites in spectrin are filled.

Besides an indirect modulation by calcium through calmodulin and calpain, which has been suggested to regulate the stability of the spectrin-based membrane skeleton (Seubert *et al.*, 1987; Harris *et al.*, 1990), it is possible that calcium can exert a direct effect through binding to the EF-hands. At present, we can only speculate on the function of the EF-hands in spectrin. Since the calcium-binding sites are located opposite to the actin- and protein 4.1-binding sites on β-spectrin in the heterodimer, it is possible that the calcium-induced conformational change influences the association of these proteins. It is also possible that calcium binding and the concomitant change in structure are transmitted to the linker region between the two EF-hands. This region seems to be important for formation and stability of the heterodimer (Viel & Branton, 1994). Another possibility is that upon massive calcium influx, calcium is bound to spectrin, and when the calcium signal diminishes, the calcium ions slowly leak from the sites on spectrin. In such a case, spectrin could function as a calcium buffer and would therefore prolong the transient calcium signal, thus allowing other calcium-binding proteins to stay activated even after the calcium transient has disappeared.

ACKNOWLEDGMENT

We are grateful to Dr. Walter Gratzer for very helpful discussions, to Dr. Annalisa Pastore and Dr. Gilles Travé for sharing their data with us, and to Dr. Paul Geladi and Mr. Eigil Dåbakk for helping with factor analysis. The technical expertise of Mrs. Eva-Maj Hägglöf is greatly appreciated.

APPENDIX

Sequential Model. In this model, it is assumed that the ligand binds in an ordered fashion:

$$P + 2X \overset{K_I}{\rightleftharpoons} PX + X \overset{K_{II}}{\rightleftharpoons} XPX$$

The microscopic association constants K_I and K_{II} are defined by

$$K_I = \frac{[PX]}{[P][X]}$$

$$KII = \frac{[XPX]}{[PX][X]}$$

The conservation of masses gives

$$[X]_{total} = 2[XPX] + [PX] + [X]$$

$$[P]_{total} = [XPX] + [PX] + [P]$$

where $[X]_{total}$ and $[P]_{total}$ denote the total concentrations of ligand and protein, respectively. The fractional saturation of the two sites is given by

$$\alpha_1 = \frac{[PX] + [XPX]}{[P]_{total}}$$

$$\alpha_2 = \frac{[XPX]}{[P]_{total}}$$

Using these equations, it is possible to express α_1 and α_2 in terms of the total concentrations of ligand and protein, and the two association constants:

$$\alpha_1 = \{K_I([X_{total}] - (\alpha_1 + \alpha_2)[P]_{total}) + K_I K_{II}([X_{total}] - (\alpha_1 + \alpha_2)[P]_{total})^2\}/\{1 + K_I([X_{total}] - (\alpha_1 + \alpha_2)[P]_{total}) + K_I K_{II}([X_{total}] - (\alpha_1 + \alpha_2)[P]_{total})^2\}$$

$$\alpha_2 = \{K_I K_{II}([X_{total}] - (\alpha_1 + \alpha_2)[P]_{total})^2\}/\{1 + K_I([X_{total}] - (\alpha_1 + \alpha_2)[P]_{total}) + K_I K_{II}([X_{total}] - (\alpha_1 + \alpha_2)[P]_{total})^2\}$$

To fit α_1 and α_2 to the experimentally determined fractional saturation of binding, the variable parameters K_I and K_{II} were varied to minimize the error of sum of squares given by

$$ESS = \sum_i (\alpha_1^{calculated} - \alpha_1^{measured})^2 + (\alpha_2^{calculated} - \alpha_2^{measured})^2$$

For this purpose, α_1 and α_2 were solved iteratively for each titration point. The iterations were done in Microsoft Excel, version 7, using the add-in tool Solver.

Two Independent Sites and Cooperative Models. In these models, it is assumed that the reactions can be described as

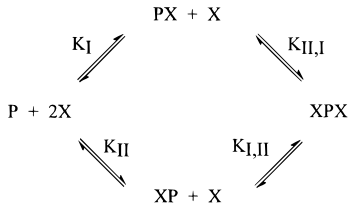

The microscopic association constants, K_I and K_{II}, are defined as

$$K_I = \frac{[PX]}{[P][X]}$$

$$K_{II} = \frac{[XP]}{[P][X]}$$

and the disproportionation equilibrium constant, K_c, is defined according to Weber (1975) as

$$K_c = \frac{[XPX][P]}{[PX][XP]}$$

By definition, K_c equals 1 when the two sites are independent and thus shows no cooperativity.

Again, the conservation of masses yields

$$[X]_{total} = 2[XPX] + [PX] + [XP] + [X]$$

$$[P]_{total} = [XPX] + [PX] + [XP] + [P]$$

In the two-site and cooperative models, the fractional saturation is given by

$$\alpha_1 = \frac{[PX] + [XPX]}{[P]_{total}}$$

$$\alpha_2 = \frac{[XP] + [XPX]}{[P]_{total}}$$

α_1 and α_2 can be expressed in $[X]_{total}$, $[P]_{total}$, K_I, K_{II}, and K_c as

$$\alpha_1 = \{K_I([X]_{total} - (\alpha_1 + \alpha_2)[P]_{total}) + K_c K_I K_{II}([X]_{total} - (\alpha_1 + \alpha_2)[P]_{total})^2\}/\{1 + (K_I + K_{II}) \times ([X]_{total} - (\alpha_1 + \alpha_2)[P]_{total}) + K_c K_I K_{II}([X]_{total} - (\alpha_1 + \alpha_2)[P]_{total})^2\}$$

$$\alpha_2 = \{K_{II}([X]_{total} - (\alpha_1 + \alpha_2)[P]_{total}) + K_c K_I K_{II}([X]_{total} - (\alpha_1 + \alpha_2)[P]_{total})^2\}/\{1 + (K_I + K_{II}) \times ([X]_{total} - (\alpha_1 + \alpha_2)[P]_{total}) + K_c K_I K_{II}([X]_{total} - (\alpha_1 + \alpha_2)[P]_{total})^2\}$$

The functions were solved iteratively for each titration point by adjusting the variable parameters K_I, K_{II}, and K_c to minimize the error of the sum of squares. When the experimental data were analyzed according to the two independent site model, the disproportionation equilibrium constant, K_c, was set to 1.

REFERENCES

Babu, Y. S., Sack, J. S., Greenhough, T. J., Bugg, C. E., Means, A. R., & Cook, W. J. (1985) *Nature 315*, 37−40.
Backman, L. (1996) *Cell. Mol. Biol. Lett. 1*, 35−48.
Bennett, V. (1990) *Phys. Rev. 70*, 1029−1065.
Berglund, Å., Backman, L., & Shanbhag, V. P. (1986) *FEBS Lett. 201*, 306−310.
Berridge, M. J. (1993) *Nature 361*, 315−325.
Björk, J., Lundberg, S., & Backman, L. (1995) *Eur. J. Cell Biol. 66*, 200−204.
Carroll, J., & Chang, J. (1970) *Psychometrika 35*, 283−319.

Chazin, W. J. (1995) *Nat. Struct. Biol. 2*, 707−710.
Chiancone, E., Thulin, E., Boffi, A., Forsén, S., & Brunor, M. (1986) *J. Biol. Chem. 261*, 16306−16308.
Clapham, D. E. (1995) *Cell 80*, 259−268.
Di Stasi, A.-M. M., Gallo, V., Ceccarini, M., & Petrucci, T. C. (1991) *Neuron 6*, 445−454.
Fox, J. E. B., Reynolds, C. C., Morrow, J. S., & Phillips, D. R. (1987) *Blood 69*, 537−545.
Gagné, S. M., Tsuda, S., Li, M. X., Smillie, L. B., & Sykes, B. D. (1995) *Nat. Struct. Biol. 2*, 784−789.
Gill, S. C., & von Hippel, P. H. (1989) *Anal. Biochem. 182*, 319−326.
Harris, A. S., & Morrow, J. S. (1990) *Proc. Natl. Acad. Sci. U.S.A. 87*, 3009−3013.
Harris, A. S., Croall, D. E., & Morrow, J. S. (1988) *J. Biol. Chem. 263*, 15754−15761.
Harris, A. S., Croall, D. E., & Morrow, J. S. (1989) *J. Biol. Chem. 264*, 17401−17408.
Hughes, C. A., & Bennett, V. (1995) *J. Biol. Chem. 270*, 18990−18996.
Karjalainen, E. (1989) *Chemom. Intell. Lab. Syst. 7*, 31−38.
Karjalainen, E., & Karjalainen, U. (1996) *Data Analysis for Hyphenated Techniques*, Elsevier, Amsterdam.
Kay, L. E., Keifer, P., & Saarinen, T. (1992) *J. Am. Chem. Soc. 114*, 10663−10665.
Knorr, F., & Futrell, J. (1979) *Anal. Chem. 51*, 1236−1241.
Kretsinger, R. H., Tolbert, D., Nakayama, S., & Pearson, W. (1991) *in Novel Calcium-Binding Proteins, Fundamental and Clinical Implications* (Heizmann, C. W., Ed.) pp 17−37, Springer Verlag, Berlin.
Lawton, W., & Sylvestre, E. (1971) *Technometrics 13*, 617−633.
Li, M. X., Gagné, S. M., Tsuda, S., Kay, C. M., Smillie, L. B., & Sykes, B. D. (1995) *Biochemistry 34*, 8330−8340.
Linse, S., & Forsén, S. (1995) *Adv. Second Messenger Phosphoprotein Res. 30*, 89−151.
Linse, S., Helmersson, A., & Forsén, S. (1991) *J. Biol. Chem. 266*, 8050−8054.
Lundberg, S., & Backman, L.(1994) *Methods Enzymol. 228*, 241−254.
Lundberg, S., Lehto, V.-P., & Backman, L. (1992) *Biochemistry 31*, 5665−5671.
Lundberg, S., Björk, J., Löfvenberg, L., & Backman, L. (1995) *Eur. J. Biochem. 230*, 658−665.
Malinovski, E. D. (1991) *Factor analysis in chemistry*, 2nd ed., Wiley-Inerscience, New York.
Mårtensson, L.-G., Jonasson, P., Freskgård, P.-O., Svensson, M., Carlsson, U., & Jonsson, B.-H. (1995) *Biochemistry 34*, 1011−1021.
McPahlen, C. A., Strynadka, N. C. J., & James, M. N. G. (1991) *Adv. Protein Chem. 42*, 77−144.
Mische, S. M., Mooseker, M. S., & Morrow, J. S. (1987) *J. Cell Biol. 105*, 2837−2845.
Moon, R. T., & McMahon, A. P. (1990) *J. Biol. Chem. 265*, 4427−4433.
Payne, M. R., & Rudnick, S. E. (1989) *Trends Biochem. Sci. 14*, 357−360.
Pedigo, S., & Shea, M. A. (1995) *Biochemistry 34*, 10676−10689.
Pietrobon, D., Di Virgilio, F., & Pozzan, T. (1990) *Eur. J. Biochem. 193*, 599−622.
Piotto, M., Saudek, V., & Sklenar, V. (1992) *J. Biomol. NMR 2*, 661−664.
Procyshyn, R. M., & Reid, R. E. (1994a) *J. Biol. Chem. 269*, 1641−1647.
Procyshyn, R. M., & Reid, R. E. (1994b) *Arch. Biochem. Biophys. 311*, 425−429.
Saido, T. C., Sorimachi, H., & Suzuki, K. (1994) *FASEB J. 8*, 814−822.
Sands, R., & Young, F. (1980) *Psychometrika 45*, 39−67.
Schägger, H., & von Jagow, G. (1987) *Anal. Biochem. 166*, 368−379.
Seubert, P., Baudry, M., Dudek, S., & Lynch, G. (1987) *Synapse 1*, 20−24.
Siman, R., Baudry, M., & Lynch, G. (1984) *Proc. Natl. Acad. Sci. U.S.A. 81*, 3572−3576.
Siman, R., Noszek, J. C., & Kegerise, C. (1989) *J. Neurosci. 9*, 1579−1590.
Starovasnik, M. A., Davis, T. N., & Klevit, R. E (1993) *Biochemistry 32*, 3261−3270.
Strynadka, N. C. J., & James, M. N. G. (1989) *Annu. Rev. Biochem. 58*, 951−998.
Strynadka, N. C. J., & James, M. N. G. (1991) *Curr. Opin. Struct. Biol. 1*, 905−914.
Travé, G., Lacombe, P.-J., Pfuhl, M., Saraste, M., & Pastore, A.-L. (1995a) *EMBO J. 14*, 4922−4931.
Travé, G., Pastore, A., Hyvönen, M., & Saraste, M. (1995b) *Eur. J. Biochem. 227*, 35−42.
Viel, A., & Branton, D. (1994) *Proc. Natl. Acad. Sci. U.S.A. 91*, 10839−10843.
Viel, A., & Branton, D. (1996) *Curr. Opin. Cell Biol. 8*, 49−55.
Wallis, C. J., Babitch, J., & Wenegieme, E. F. (1993) *Biochemistry 32*, 5045−5050.
Wasenius, V.-M., Saraste, M., Salvén, P., Erämaa, M., Holm, L., & Lehto, V.-P. (1989) *J. Cell Biol. 109*, 79−93.
Weber, G. (1975) *Adv. Protein Chem. 29*, 1−83.
Woody, R. W. (1995) *Methods Enzymol. 246*, 35−71.
Zhang, M., Tanaka, T., & Ikura, M. (1995) *Nat. Struct. Biol. 2*, 758−767.

BI9631531